ARCHIVES OF ACOUSTICS
20, 3, 247–269 (1995)

PROPAGATION AND SCATTERING OF APM IN THE PIEZOELECTRIC PLATE WITH PERIODICALLY CORRUGATED SURPHACES

D. BOGUCKI
Institute of Fundamental Technological Research
Polish Academy of Sciences
(00–049 Warszawa, Świętokrzyska 21)

Bragg reflection of acoustic plate modes (APM) in piezoelectric plate with periodically grooved surfaces is analysed. Reflectional mode conversion and phenomena of APM propagation along the grooves are also taken into account. Influence of phase shift between the grooves on dispersion relations is also analysed. Presented results may be applied in the analysis of APM sensors and signal processing devices.

1. Introduction

Phenomena of SAW propagation in a piezoelectric substrate with periodically corrugated surface were analysed in details in literature [5], [8], [11]. Corrugation has, usually, a form of shallow, periodic grooves. In this case, in substrate propagates one surface mode [5], [9] and the Bragg condition has the form $K=2k_v$, where K is wavenumber of grooves system and k_v is SAW wavenumber.

Corresponding phenomena in the piezoelectric plate are more complicated because of multimodal propagation of acoustic plate modes (APM) [2], [3], [4]. Different modes may be coupled by formula:

$$\mathbf{K}=\mathbf{k}_f=\mathbf{k}_b,$$

where: $\mathbf{k}_f$ — wavevector of forwards propagating mode, $\mathbf{k}_b$ — is wavevector of backwards propagating mode. In the coupling of different modes we have also phenomena of reflectional mode conversion.

If the plate is corrugated on both sides, then reflection of different modes, depends on grooves amplitude and their phase shift.

Different phenomenon is APM propagation along the grooves. There is no Bragg reflection in this case — propagation has a form of waveguiding by grooves of corrugation. This effect is similar to a SAW propagation along the grooves deposited on the isotropic halfspace analysed by A.A. MARADUDIN *et al.* in [11] and [12].

APM propagation in the isotropic corrugated plates was analysed by author in [10].

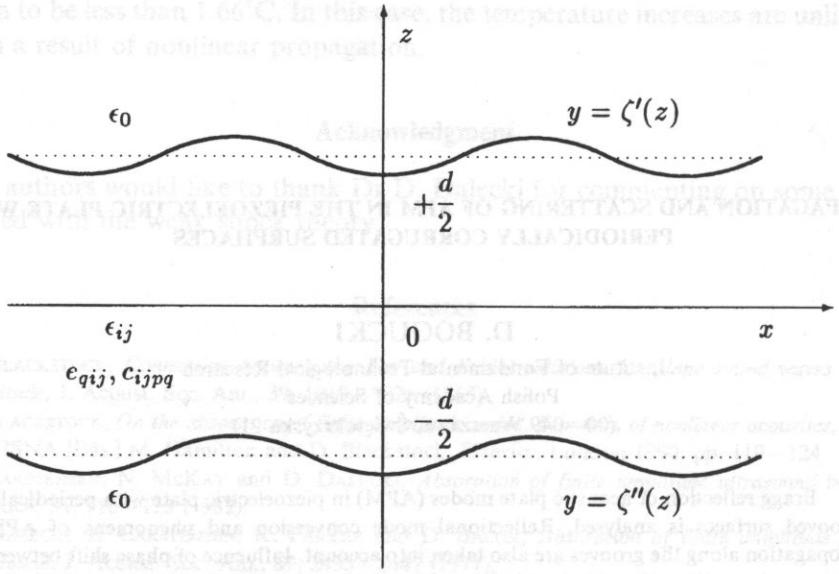

Fig. 1. Piezoelectric plate corrugated on both surfaces

In this paper APM propagation in the piezoelectric plate with both surfaces periodically corrugated is analysed. Solution for plate with corrugated one surface may be easily obtained from this generalized case. We consider slant propagating wave (with reference to groove system) and propagation of APM along the grooves in infinite piezoelectric plate d — thick (Fig. 1). Piezoelectric plate is characterised by ρ-mass density and material tensors ϵ_{ij}, e_{qij}, c_{ijpq}. Below and above the plate there is vacuum (ϵ_0). Periodic corrugation may be described as follows:

$$\zeta'(z) = h_1 e^{-jKz} + h_1^* e^{jKz}, \tag{1.1}$$

$$\zeta''(z) = h_2 e^{-jKz} + h_2^* e^{jKz}, \tag{1.2}$$

where $\Lambda = 2\pi/K$ is a period of corrugation. Corrugation amplitudes h_1, h_2 may be different, they especially may be phase shifted. Corrugation is assumed to be small, so a perturbation theory may be applied:

$$\left|\frac{h_i}{\Lambda}\right| \ll 1, \quad \left|\frac{h_i}{d}\right| \ll 1 \quad i = 1, 2. \tag{1.3}$$

We consider waves propagating in any direction on a (x, z) plane. According to the Floquet theorem [6], solutions for displacements and stresses in the structure may be written in the form:

$$T_{il} = \sum_n T_{il}^{(n)} e^{-j(s+nK)z} e^{-jrx} e^{j\omega t}, \tag{1.4}$$

$$u_i = \sum_n u_i^{(n)} e^{-j(s+nK)z} e^{-jrx} e^{j\omega t}, \tag{1.5}$$

where $i, j = x, y, z$ and $r > 0$, $s > 0$ — wave vector components of the incident wave in x and z axis direction respectively (Fig. 2). Analogous assumptions are made for electric field flux density and electric potential inside the plate:

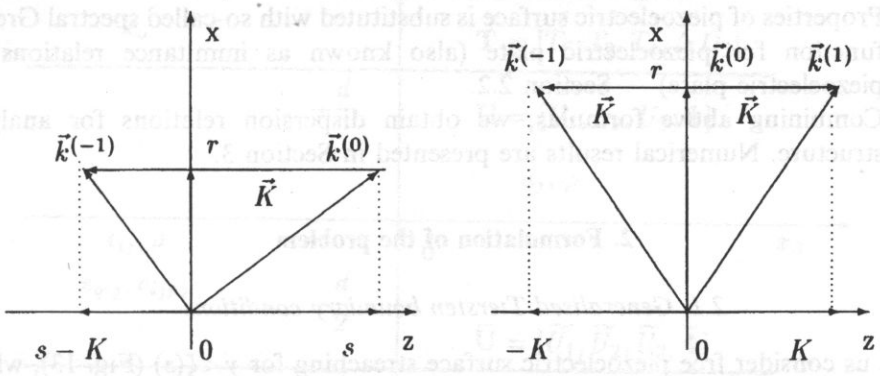

Fig. 2. Wavevectors taken into consideration in analysis: left — for oblique incidence, right — for propagation along the grooves.

$$D_i = \sum_n D_i^{(n)} e^{-j(s+nK)z} e^{-jrx} e^{j\omega t}, \tag{1.6}$$

$$\varphi = \sum_n \varphi^{(n)} e^{-j(s+nK)z} e^{-jrx} e^{j\omega t}, \tag{1.7}$$

Electric potential over and below the plate must additionally dissapear in $+\infty$ and in $-\infty$ respectively:

$$\varphi' = \sum_n \varphi'^{(n)} e^{-j(s+nK)z} e^{-jrx} e^{-k(n)y} e^{j\omega t}, \tag{1.8}$$

$$\varphi'' = \sum_n \varphi''^{(n)} e^{-j(s+nK)z} e^{-jrx} e^{-k(n)y} e^{j\omega t}, \tag{1.9}$$

where $k^{(n)} = \sqrt{r^2 + (s+nK)^2}$. In the case of slant propagating waves (with reference to the groove system) only the lowest harmonic components, coupled by Bragg condition are taken into account i.e. $n = 0, -1$. For propagation along the grooves (eg. for $s = 0$), it is necessary to account components $n = -1, 0, 1$, because $k^{(1)} = k^{(-1)}$.

This simplification is allowed in presented perturbation analysis ($h_i \to 0$). For $|n| \to \infty$ solutions for u_i and φ describe leaky modes exponentially attenuated with distance from plate surfaces. These modes gives ommitable contribution in total energy and can be neglected.

In this paper are analysed dispersion relations i.e. relations between ω and wavevector components s, r. Method of solution is the same for plate corrugated on one or on both surfaces:

1. Structure is decomposed onto three (two) parts:
   - Piezoelectric plate d-thick

- Thin, corrugated piezoelectric layers h_i — thick.

2. Influence of corrugated surfaces is substituted with so-called generalized Tiersten boundary conditions — Section 2.1.
3. Properties of piezoelectric surface is substituted with so-called spectral Green's function for piezoelectric plate (also known as immitance relations for piezoelectric plate) — Section 2.2.
4. Combining above formulas, we obtain dispersion relations for analysed structure. Numerical results are presented in Section 3.

2. Formulation of the problem

2.1. Generalised Tiersten boundary conditions

Let us consider free piezoelectric surface streaching for $y<\zeta(z)$ (Fig. 13), where

$$\zeta(z)=he^{-jKz}+h^*e^{jKz} \tag{2.1}$$

describes sinusoidally grooved surface with period $\Lambda=2\pi/K$ and amplitude $h\ll\Lambda$ (grooves are parallel to the x-axis). In [8] were presented so-called generalized Tiersten boundary conditions. They were exploited in the analysis of periodically corrugated isotropic plate in [10].

Generalised Tiersten boundary conditions have the form of additional stresses and electric charges subjected to mean surface $y=0$, in the function of known displacements and electric potential on the same surface. On the other hand, generalized Tiersten boundary conditions replace homogeneous boundary conditions on corrugated surface by inhomogeneous boundary conditions on mean surface (in simplification of small corrugation). In our case they have general form (denotation of complex amplitudes is analogous to (1.4)–(1.7).

$$\mathbf{T}^{(n)}=h\mathbf{g}^{(n,n-1)}\cdot\mathbf{U}^{(n-1)}+h^*\mathbf{g}^{(n,n+1)}\cdot\mathbf{U}^{(n+1)}, \tag{2.2}$$

where

$$\mathbf{T}^{(n)}\equiv[T_6^{(n)};T_2^{(n)};T_4^{(n)};\Delta D_2^{(n)}] \quad \text{and} \quad \mathbf{U}^{(n)}\equiv[u_1^{(n)};u_2^{(n)};u_3^{(n)};\varphi^{(n)}].$$

It is worth to note that in above formulas, matrices $\mathbf{g}^{(n,n+1)}$ and $\mathbf{g}^{(n,n-1)}$ couple waves propagating with different wavenumbers (for example wave $n=0$ with $n=\pm1$). This effect disapears with $h\to0$.

Method of evaluation of mentioned relationships for piezoelectric material and two-dimensional corrugation (periodic dots) is presented in the Appendix A.

2.2. Immitance relations for piezoelectric plate

Let us consider infinite piezoelectric plate bounded by planes $x_2=\pm d/2$ (Fig. 3) made of material characterized by ρ — mass density and material constants ϵ_{ij}, e_{qij}, c_{ijpq}. Vacuum (ϵ_0) is outside the plate. We consider harmonic waves propagating in

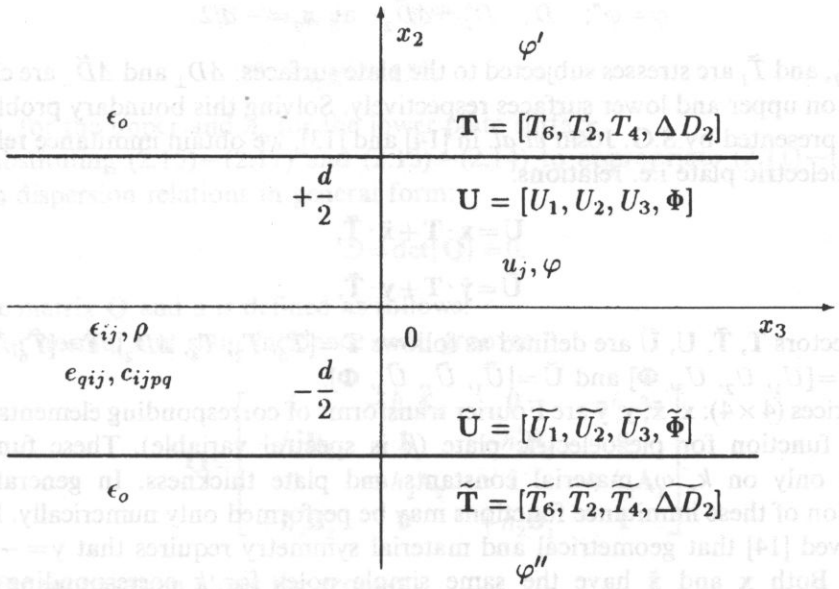

Fig. 3. Piezoelectric plate with forces on both surfaces.

x_3-axis direction proportional to $\exp(j\omega t - jkx_3)$, where k is wavenumber and ω is angular frequency.

In the piezoelectric material, the coupled acoustic wave equations are (in quasi-static approximation):

$$\begin{aligned} \rho\omega^2 u_i &= c_{ijpq}\, u_{p,jq} + e_{qij}\varphi_{,jq}, \\ 0 &= e_{jpq}\, u_{p,jq} - \epsilon_{jq}\, \varphi_{,jq}, \end{aligned} \tag{2.3}$$

where u_p is the particle displacement in the p-axis direction and φ is the electric potential inside the plate. Electric potential above (φ') and below (φ'') the plate satisfy Laplace's equation in the vacuum:

$$\begin{aligned} 0 &= \varphi'_{,jj}, \\ 0 &= \varphi''_{,jj}. \end{aligned} \tag{2.4}$$

Appropriate electrical and mechanical conditions must be satisfied on both plate surfaces. The mechanical boundary conditions are

$$T_{2i} = T_I \quad \text{at } x_2 = +d/2, \tag{2.5}$$

$$T_{2i} = T_I \quad \text{at } x_2 = -d/2, \tag{2.6}$$

and the electrical ones:

$$\varphi = \varphi'; \quad D_2 - D'_2 = \Delta D_2 \quad \text{at } x_2 = +d/2, \tag{2.7}$$

$$\varphi=\varphi''; \quad D_2-D_2''=\Delta\tilde{D}_2 \quad \text{at } x_2=-d/2, \tag{2.8}$$

where T_I, and $\tilde{T}_I$ are stresses subjected to the plate surfaces. $\Delta D_\perp$ and $\Delta\tilde{D}_\perp$ are charges induced on upper and lower surfaces respectively. Solving this boundary problem, in the way presented by S.G. Joshi *et al.* in [14] and [13], we obtain immitance relations for piezoelectric plate i.e. relations:

$$\mathbf{U}=\mathbf{x}\cdot\mathbf{T}+\tilde{\mathbf{x}}\cdot\tilde{\mathbf{T}}, \tag{2.9}$$

$$\tilde{\mathbf{U}}=\tilde{\mathbf{y}}\cdot\mathbf{T}+\mathbf{y}\cdot\tilde{\mathbf{T}}, \tag{2.10}$$

where vectors $\mathbf{T}$, $\tilde{\mathbf{T}}$, $\mathbf{U}$, $\tilde{\mathbf{U}}$ are defined as follows $\mathbf{T}=[T_6, T_2, T_4, \Delta D_2]$, $\tilde{\mathbf{T}}=[\tilde{T}_6, \tilde{T}_2, \tilde{T}_4, \Delta\tilde{D}_2]$, $\mathbf{U}=[U_1, U_2, U_3, \boldsymbol{\Phi}]$ and $\tilde{\mathbf{U}}=[\tilde{U}_1, \tilde{U}_2, \tilde{U}_3, \boldsymbol{\Phi}]$.

Matrices (4×4): $\mathbf{x}$, $\tilde{\mathbf{x}}$, $\mathbf{y}$, $\tilde{\mathbf{y}}$ are Fourier transforms of corresponding elements of the Green's function for piezoelectric plate (k is spectral variable). These functions depends only on k, ω, material constants and plate thickness. In general case, calculation of these immitance functions may be performed only numerically. It may be prooved [14] that geometrical and material symmetry requires that $\mathbf{y}=-\mathbf{x}$ and $\tilde{\mathbf{y}}=-\tilde{\mathbf{x}}$. Both $\mathbf{x}$ and $\tilde{\mathbf{x}}$ have the same simple poles for k corresponding APM wavenumber. Matrix $\mathbf{x}$ is hermitian ($x_{ij}=x_{ji}^*$), and $\tilde{\mathbf{x}}$ is symmetrical ones ($x_{ij}=x_{ji}$) [14], [13].

Matrices $\mathbf{x}$ and $\tilde{\mathbf{x}}$ for isotropic plate were presented in [10]. It is worth to note that only for piezoelectric materials elements x_{i4} and $\tilde{x}_{i4}$ are non equal to zero, because they describe coupling between mechanical displacements and electric field.

2.3. *Dispersion relations*

Let us introduce for each n new coordinate system such that axis $y\equiv x_2^{(n)}$ and $x_3^{(n)}\equiv k^{(n)}$ (Figure 2). Immitance relations for each n have the form:

$$\mathbf{U}^{(n)}=\mathbf{x}^{(n)}\cdot\mathbf{T}^{(n)}+\tilde{\mathbf{x}}^{(n)}\cdot\tilde{\mathbf{T}}^{(n)}, \tag{2.11}$$

$$\tilde{\mathbf{U}}^{(n)}=-\tilde{\mathbf{x}}^{(n)}\cdot\mathbf{T}^{(n)}-\mathbf{x}^{(n)}\cdot\tilde{\mathbf{T}}^{(n)}. \tag{2.12}$$

Transforming in the same way generalized Tiersten conditions and taking into account only the lowest harmonic components, coupled by Bragg condition we obtain (Section 1):

- for normal nad slant incidence onto grooves i.e. taking into account $n=0, -1$ we have:

$$\mathbf{T}^{(0)}=h_i\,\mathbf{g}^{(0,-1)}\cdot\mathbf{U}^{(-1)}, \tag{2.13}$$

$$\mathbf{T}^{(-1)}=h_i^*\,\mathbf{g}^{(-1,0)}\cdot\mathbf{U}^{(0)}, \tag{2.14}$$

- propagation along the grooves i.e. taking into account $n=1, 0, -1$ we have:

$$\mathbf{T}^{(0)}=h_i\,\mathbf{g}^{(0,-1)}\cdot\mathbf{U}^{(-1)}+h_i^*\,\mathbf{g}^{(0,1)}\cdot\mathbf{U}^{(1)}, \tag{2.15}$$

$$\mathbf{T}^{(-1)}=h_i^*\,\mathbf{g}^{(-1,0)}\cdot\mathbf{U}^{(0)}, \tag{2.16}$$

$$\mathbf{T}^{(1)}=h_i\,\mathbf{g}^{(1,0)}\cdot\mathbf{U}^{(0)}, \tag{2.17}$$

h_i is h_1 for the upper and h_2 for the lower plate surface.

Substituting (2.15)–(2.17) and (2.13)–(2.14) to appropriate (2.11)–(2.12) we obtain dispersion relations in general form:

$$D=\det\{\mathbf{Q}\}=0. \tag{2.18}$$

Where matrix $\mathbf{Q}$ and $\mathbf{u}$ is defined as follows:

• for normal and slant incidence onto grooves

$$\mathbf{Q}=\begin{bmatrix} \mathbf{I} & -h_1\mathbf{A}_1 & \mathbf{0} & -h_1\mathbf{A}_2 \\ -h_1^*\mathbf{B}_1 & \mathbf{I} & -h_1^*\mathbf{B}_2 & \mathbf{0} \\ \mathbf{0} & +h_2\mathbf{A}_2 & \mathbf{I} & +h_2\mathbf{A}_1 \\ +h_2^*\mathbf{B}_2 & \mathbf{0} & +h_2^*\mathbf{B}_1 & \mathbf{I} \end{bmatrix}. \tag{2.19}$$

• for propagation along the grooves

$$\mathbf{Q}=\begin{bmatrix} \mathbf{I} & -h_1\mathbf{C}_1 & \mathbf{0} & \mathbf{0} & -h_1\mathbf{C}_2 & \mathbf{0} \\ -h_1^*\mathbf{D}_1 & \mathbf{I} & -h_1\mathbf{A}_1 & -h_1^*\mathbf{D}_2 & \mathbf{0} & -h_1^*\mathbf{A}_2 \\ \mathbf{0} & -h_1^*\mathbf{B}_1 & \mathbf{I} & \mathbf{0} & -h_1^*\mathbf{B}_2 & \mathbf{0} \\ \mathbf{0} & +h_2\mathbf{C}_2 & \mathbf{0} & \mathbf{I} & +h_2\mathbf{C}_1 & \mathbf{0} \\ +h_2^*\mathbf{B}_2 & \mathbf{0} & +h_2\mathbf{A}_2 & +h_2^*\mathbf{D}_1 & \mathbf{I} & +h_2\mathbf{A}_1 \\ \mathbf{0} & +h_2^*\mathbf{B}_2 & \mathbf{0} & \mathbf{0} & +h_2\mathbf{B}_1 & \mathbf{I} \end{bmatrix}. \tag{2.20}$$

$\mathbf{I}$ is unitary matrix and $\mathbf{A}_I$, $\mathbf{B}_I$, $\mathbf{C}_I$, $\mathbf{D}_I$ are 4×4 matrices defined as follows:

$$\mathbf{A}_1=\mathbf{x}^{(0)}\cdot\mathbf{g}^{(0,-1)}, \qquad \mathbf{A}_2=\tilde{\mathbf{x}}^{(0)}\cdot\mathbf{g}^{(0,-1)}, \tag{2.21}$$

$$\mathbf{B}_1=\mathbf{x}^{(-1)}\cdot\mathbf{g}^{(-1,0)}, \qquad \mathbf{B}_2=\tilde{\mathbf{x}}^{(-1)}\cdot\mathbf{g}^{(-1,0)}, \tag{2.22}$$

$$\mathbf{C}_1=\mathbf{x}^{(1)}\cdot\mathbf{g}^{(1,0)}, \qquad \mathbf{C}_1=\tilde{\mathbf{x}}^{(1)}\cdot\mathbf{g}^{(1,0)}, \tag{2.23}$$

$$\mathbf{D}_1=\mathbf{x}^{(0)}\cdot\mathbf{g}^{(0,1)}, \qquad \mathbf{D}_2=\tilde{\mathbf{x}}^{(0)}\cdot\mathbf{g}^{(0,1)}. \tag{2.24}$$

Dispersion relation for piezoelectric plate corrugated on one side may be obtained by substitution $h_2=0$ in presented above formulas.

3. Numerical results

In numerical results presented in this section it is assumed that:

• $s\in(0,K)$ i.e. s is in the first Brillouin zone;

• angular frequency ω is normalised to $\Omega=\omega/V$ and $V=\sqrt{c_{44}/\rho}$, so $\Omega\in(0,K)$;

• it is assumed that $h_i=0.01\,\Lambda$;

- place thickness d is normalised: $d=m\cdot\Lambda/2\pi$; We analyse relatively thin plates with $m=1$ because for $m>3$ higher APM may propagate and corresponding dispersion relations are much more complicated;
- $r\in(0,K)$ for the waves propagating aiong the grooves and for slowness curves.
- amplitudes of corrugation on both sides are: $h_1=h\exp\left\{-j\frac{\psi}{2}\right\}$ and $h_2=h\exp\left\{+j\frac{\psi}{2}\right\}$ i.e. are phase-shifted by ψ.

It may be easily prooved that highest frequency $f_{\max}$ of model correctness is given:

$$f_{\max}=\frac{V}{\Lambda}. \tag{3.1}$$

For $f>f_{\max}$ we must take into account more n in the series (1.4)–(1.7).

3.1. Normal and slant incidence onto grooves

We analyse equation (2.18) in a two ways:

1. For normal incidence onto the grooves i.e. for $r=0$, the most natural is to analyse dispersion relation $D(r, s, \Omega)=0$ on (s,Ω) plane.
2. For slant incidence onto the grooves more useful is to analyse slowness curves i.e. for $\Omega=$const on (r,s) plane.

Numerical results for popular piezoelectric materials (BGO, SiO_2, $LiNbO_3$) are presented on Figures 4–10. Upper part of Figures 4–9 show dispersion curves for piezoelectric plate corrugated on one side. Dotted lines are dispersion curves for free (uncorrugated $h=0$) plate. Lower part of figures, presents dispersion curves for plates with corrugates both sides.

For APM propagation in the corrugated plates, existence of forbidden frequency bands (marked with letters on Figures 4–9, see table below).

letter	reflection	letter	reflection
a	$SH_0\leftrightarrow SH_0$	d	$A_0\leftrightarrow S_0$
b	$A_0\leftrightarrow A_0$	e	$A_0\leftrightarrow SH_0$
c	$S_0\leftrightarrow S_0$	f	$S_0\leftrightarrow SH_0$

Inside those bands wavenumber has complex values — which is connected with effects of Bragg reflection. There are two kind os stopbands:

- associated with backward mode reflection (a, b, c) inside those bands $Re\{s\}=K/2=$const
- connected with reflection associated with mode conversion. In this case $Re\{s\}\neq K/2\neq$const because of different velocities of coupled modes.

Let us note that, if crystal cut of the plate is such that in analysed plate displacements in saggital plane (u_2, u_3) and u_1 are independent each other, then for

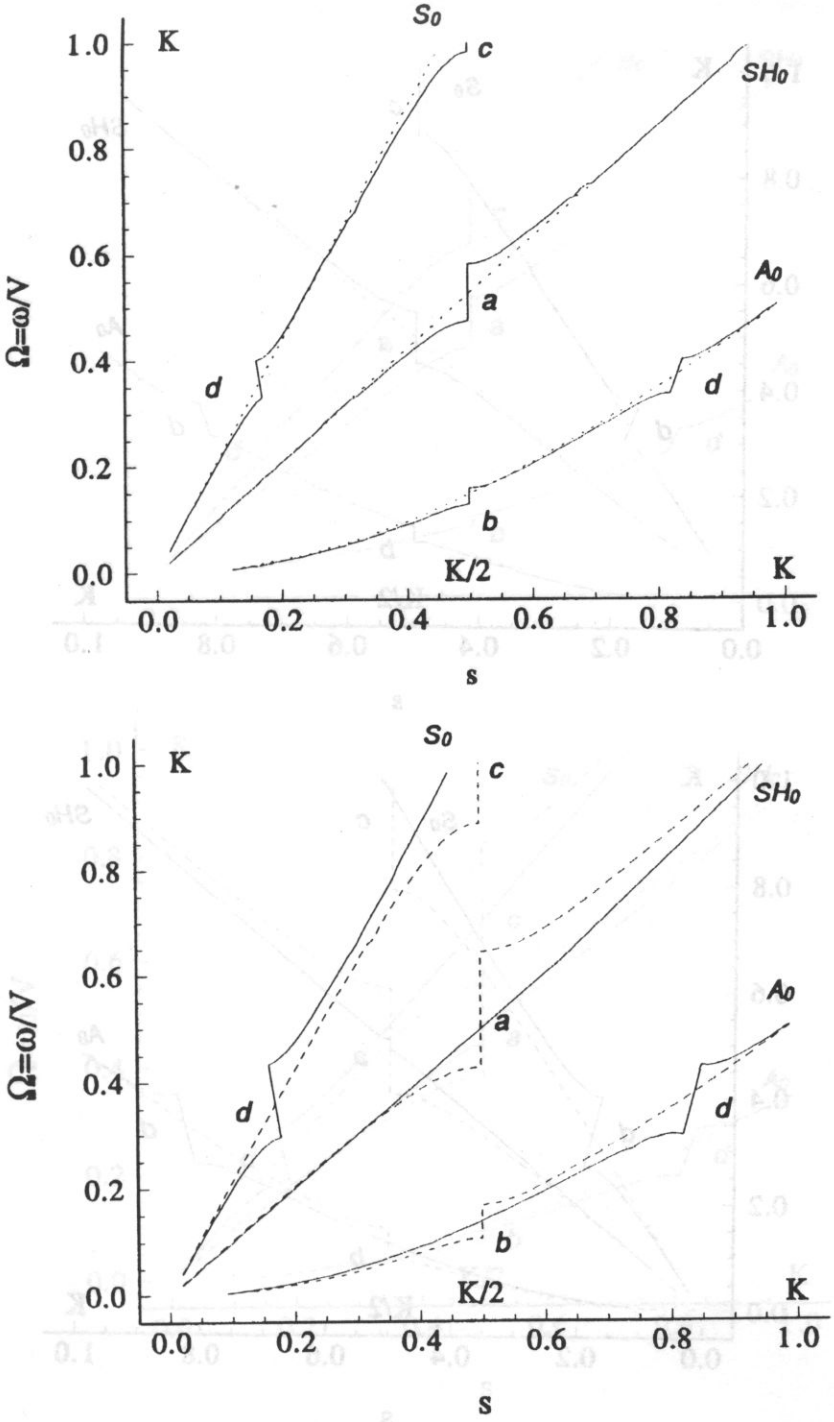

Fig. 4. BGO YZ plate $m=1$ thick, dispersion curves at $r=0$. Above: corrugated one side, dotted line — uncorrugated plate. Below: two-side corrugations phase-shifted by: a) $\psi=0$ — solid line and b) $\psi=\pi$ — dashed line.

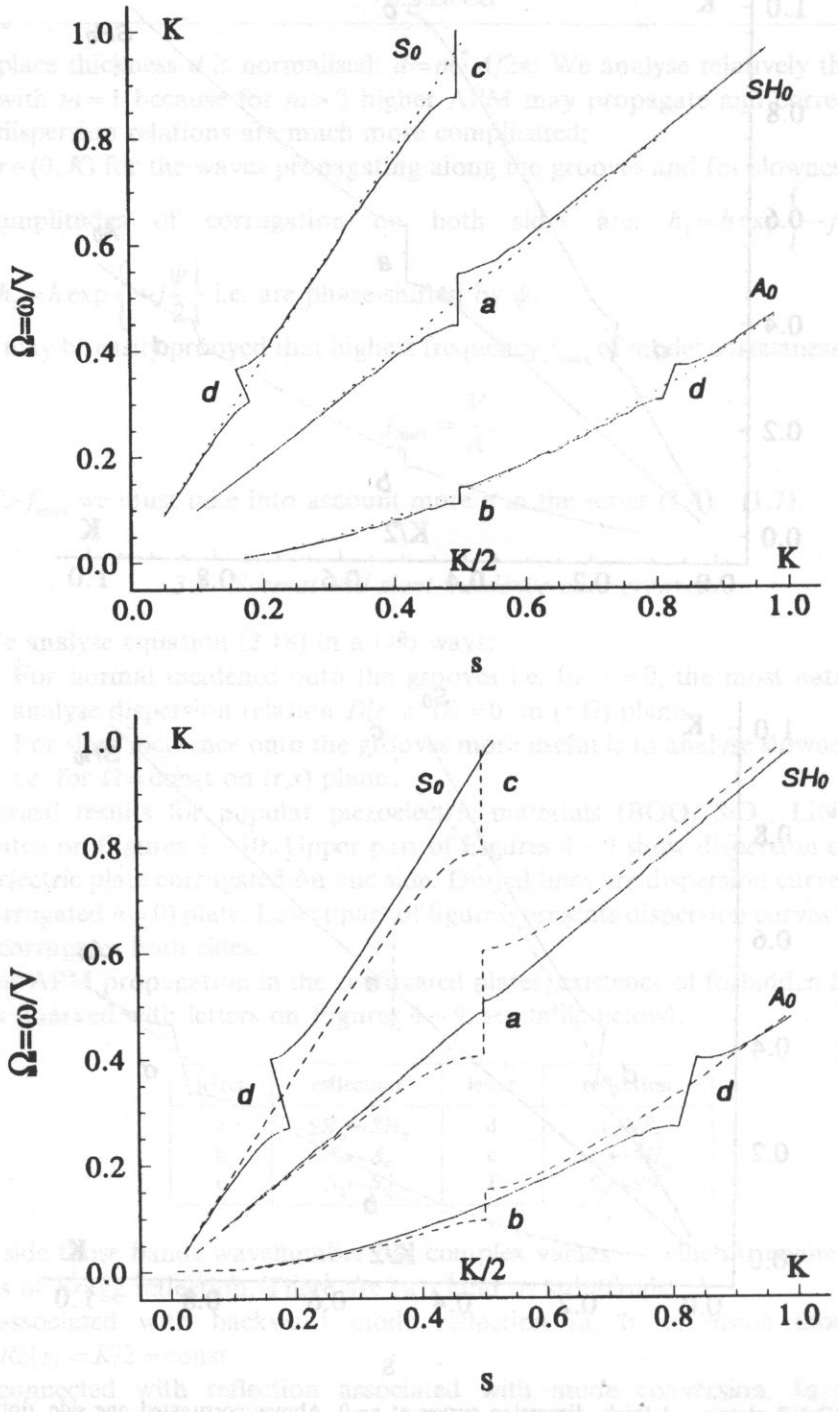

Fig. 5. $LiNbO_3$ YZ plate $m=1$ thick, dispersion curves at $r=0$. Above: corrugated one side, dotted line — uncorrugated plate. Below: two-side corrugations phase-shifted by: a) $\psi=0$ — solid line and b) $\psi=\pi$ — dashed line.

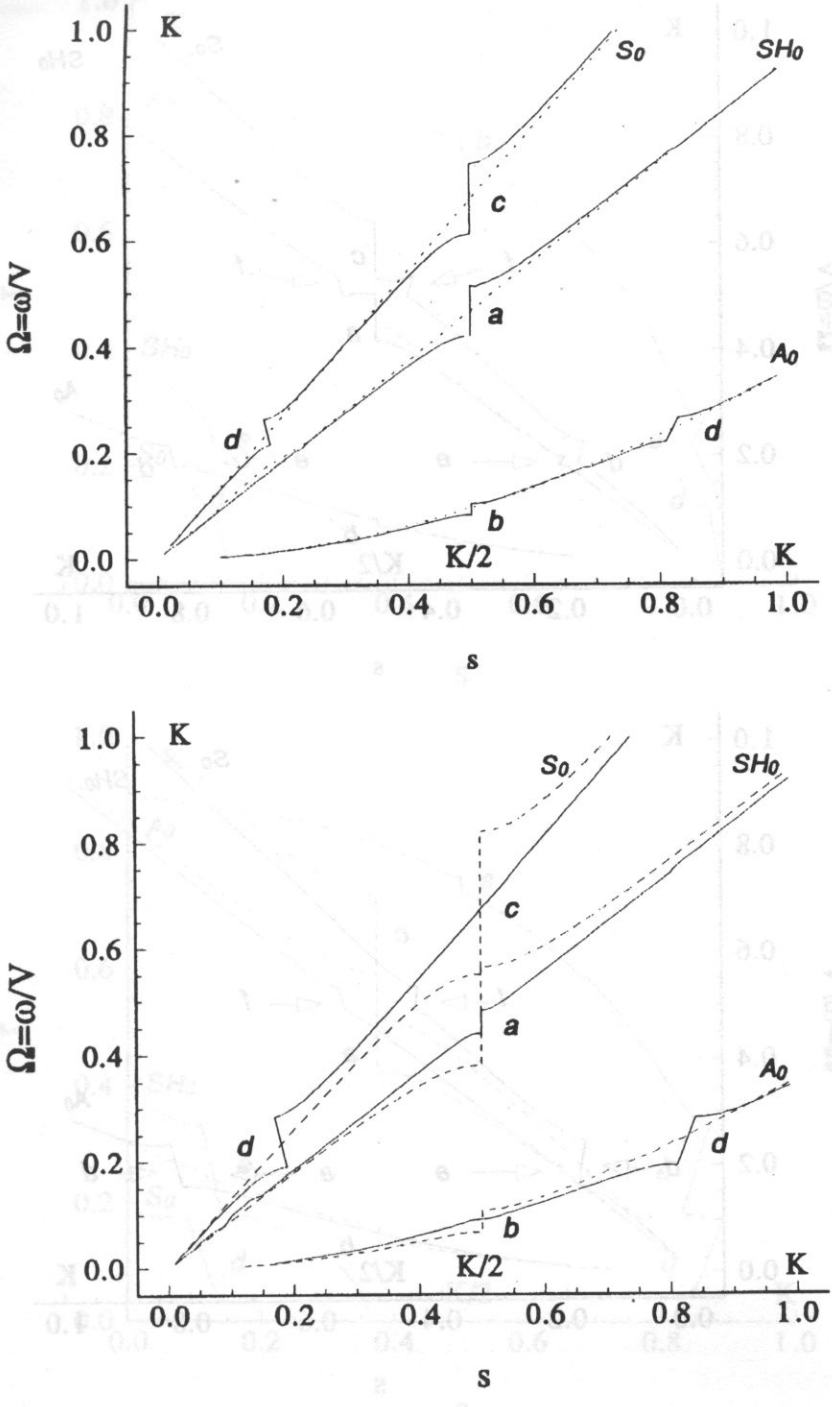

Fig. 6. SiO_2 YZ plate $m=1$ thick, dispersion curves at $r=0$. Above: corrugated one side, dotted line — uncorrugated plate. Below: two-side corrugations phase-shifted by: a) $\psi=0$ — solid line and b) $\psi=\pi$ — dashed line.

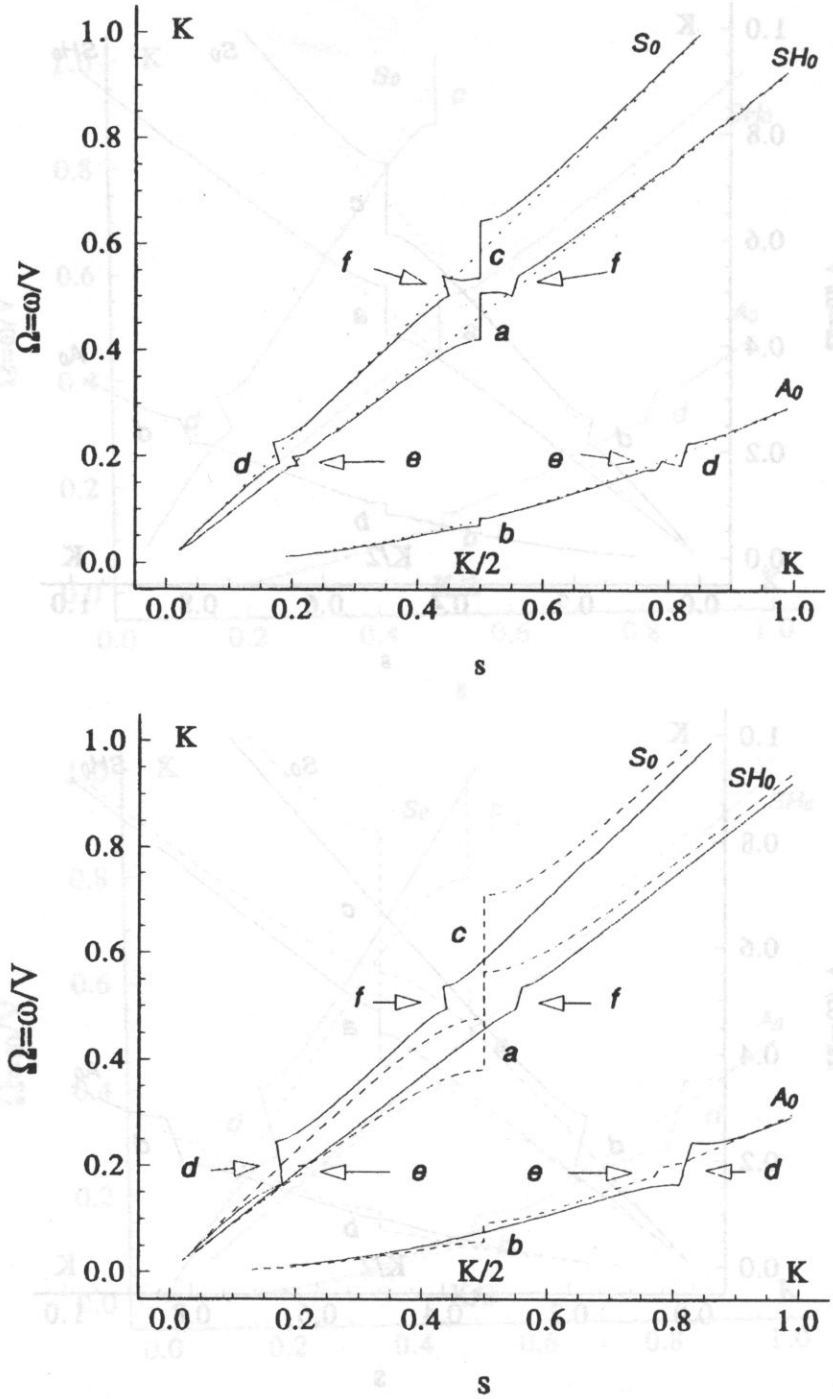

Fig. 7. SiO_2 YX plate $m=1$ thick, dispersion curves at $r=0$. Above: corrugated one side, dotted line — uncorrugated plate. Below: two-side corrugations phase-shifted by: a) $\psi=0$ — solid line and b) $\psi=\pi$ — dashed line.

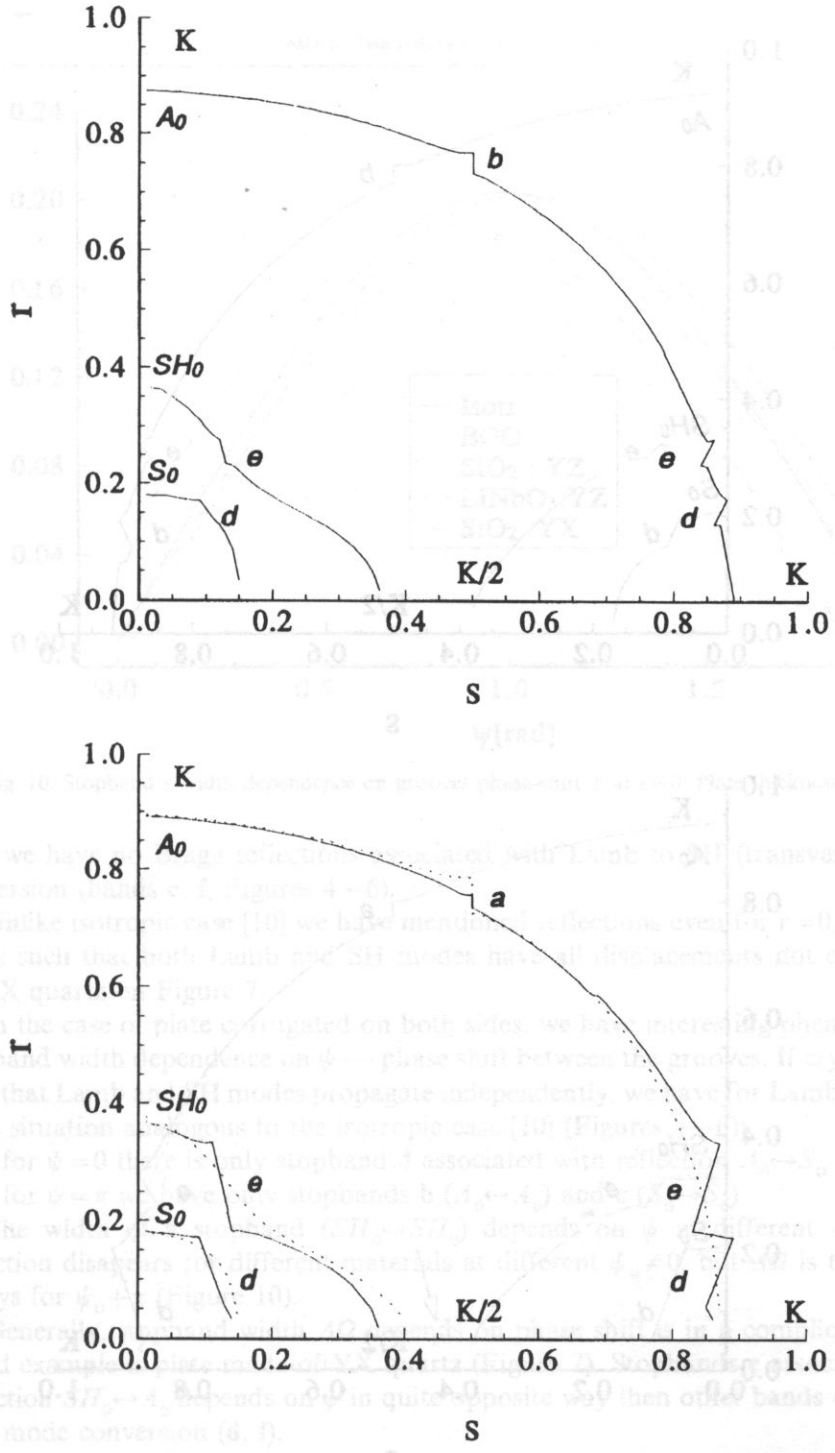

Fig. 8. Slowness curves at $\Omega=0.4$ *K*. BGO YZ plate $m=1$ thikc. Above: plate corrugated on one side. Below: two-side corrugations phase-shifted by: a) $\psi=0$ — (solid line) and b) $\psi=\pi$ — (dashed line).

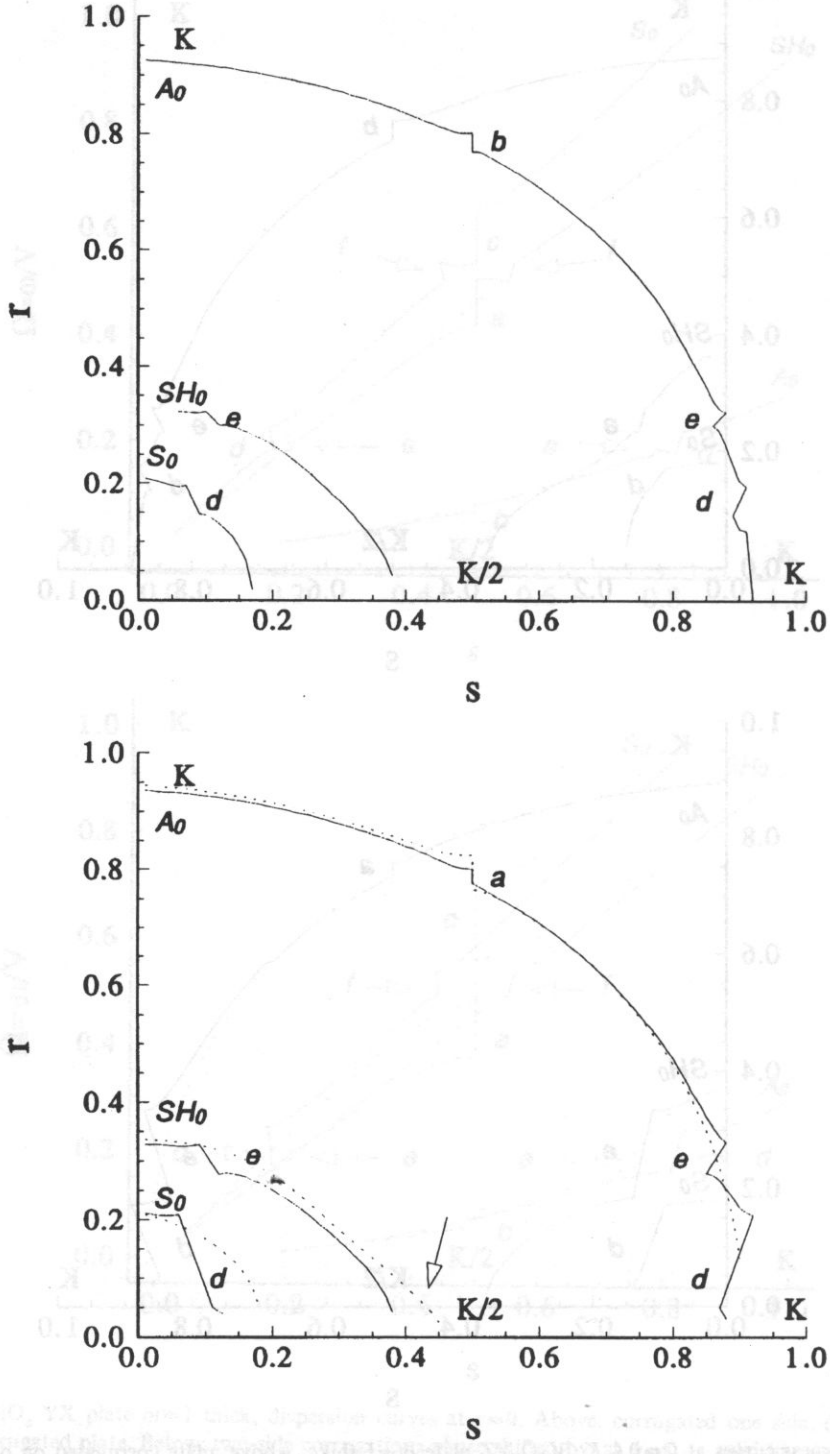

Fig. 9. Slowness curves at $\Omega = 0.4$ *K*. $LiNbO_3$ YZ plate $m = 1$ thick. Above: plate corrugated on one side. Below: two-side corrugations phase-shifted by: a) $\psi = 0$ — (solid line) and b) $\psi = \pi$ — (dashed line).

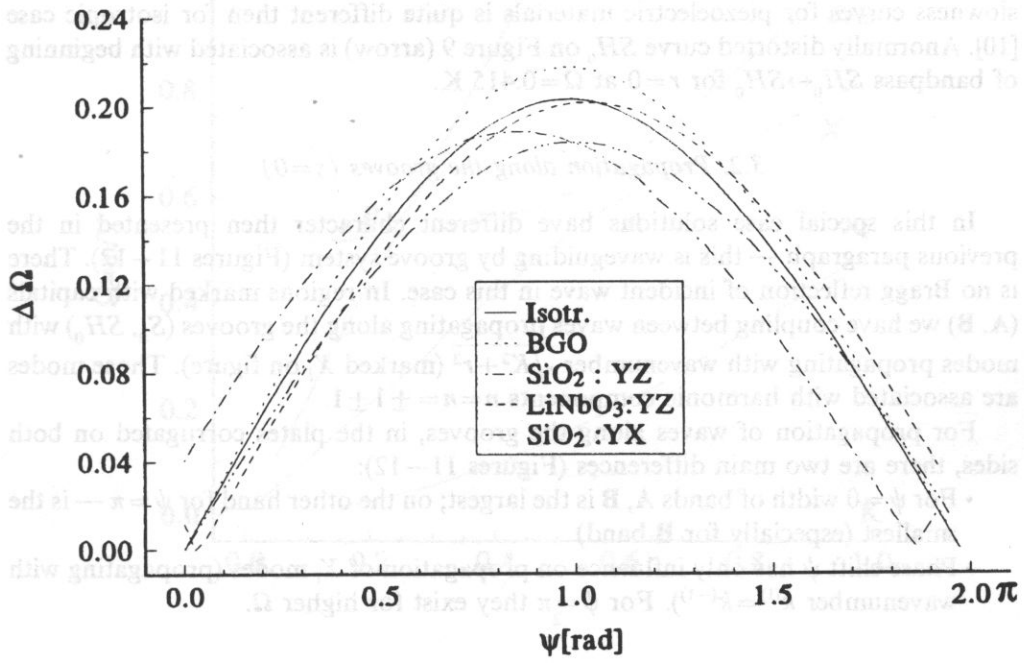

Fig. 10. Stopband a width dependence on grooves phase-shift ψ at $r=0$. Plate thickness: $m=1$.

$r=0$ we have no Bragg reflections associated with Lamb to SH (transverse) mode conversion (bands **e**, **f**, Figures 4–6).

Unlike isotropic case [10] we have mentioned reflections even for $r=0$, if crystal cut is such that both Lamb and SH modes have all displacements not equal zero — YX quartz on Figure 7.

In the case of plate corrugated on both sides, we have interesting phenomena of stopband width dependence on ψ — phase shift between the grooves. If crystal cut is such that Lamb and SH modes propagate independently, we have for Lamb modes at $r=0$, situation analogous to the isotropic case [10] (Figures 4–6):

- for $\psi=0$ there is only stopband **d** associated with reflection $A_0 \leftrightarrow S_0$
- for $\psi=\pi$ we have only stopbands **b** ($A_0 \leftrightarrow A_0$) and **c** ($S_0 \leftrightarrow S_0$)

The width of **a** stopband ($SH_0 \leftrightarrow SH_0$) depends on ψ in different way. This reflection disapears for different materials at different $\psi_0 \neq 0$, but $\Delta\Omega$ is the largest always for $\psi_0+\pi$ (Figure 10).

Generally, stopband width $\Delta\Omega$ depends on phase shift ψ in a complicated way. Good example is plate made of YX quartz (Figure 7). Stopbands **e** associated with relfection $SH_0 \leftrightarrow A_0$ depends on ψ in quite opposite way then other bands associated with mode conversion (**d**, **f**).

Numerical results for slant incidence of wave onto the grooves are presented on Figures 8, 9. In this case, analogously isotropic case [10] we have always stopbands **e**, **f** associated with reflection of SH to Lamb modes. On the other hand, the shape of

slowness curves for piezoelectric materials is quite different then for isotropic case [10]. Anormally distorted curve SH_0 on Figure 9 (arrow) is associated with beginning of bandpass $SH_0 \leftrightarrow SH_0$ for $r=0$ at $\Omega=0.415$ K.

3.2. Propagation along the grooves ($s=0$)

In this special case solutions have different character then presented in the previous paragraph — this is waveguiding by groove system (Figures 11 – 12). There is no Bragg reflection of incident wave in this case. In regions marked with capitals (**A**, **B**) we have coupling between waves propagating along the grooves (S_0, SH_0) with modes propagating with wavenumber $\sqrt{K^2+r^2}$ (marked X_i on figure). Those modes are associated with harmonic components $n=n=\pm 1 \pm 1$.

For propagation of waves along the grooves, in the plates corrugated on both sides, there are two main differences (Figures 11 – 12):

- For $\psi=0$ width of bands **A**, **B** is the largest; on the other hand for $\psi=\pi$ — is the smallest (especially for **B** band)
- Phase shift ψ has only influence on propagation of X_i modes (propagating with wavenumber $k^{(1)}=k^{(-1)}$). For $\psi=\pi$ they exist for higher Ω.

4. Conclusions

1. In piezoelectric plate with periodically corrugated surfaces, we have Bragg reflection phenomena associated with mode conversion — in this case $Re\{s\} \neq \text{const}$ inside forbidden band of frequency. This effect is caused by different velocities of coupled modes.

2. If crystal cut is such, that in plane normal to the grooves Lamb and SH modes propagate independent each other then for $r=0$ there is no reflection associated with conversion of Lamb to SH modes. This effect is possible for slant incidence of wave onto the grooves.

3. For plate with both surfaces periodically corrugated, width of stopbands depends on phase shift between corrugation grooves ψ. Changing ψ we could obtain only reflection of certain kind. Those phenomena may be useful in elimination of parasitic effects of multimodal propagation in APM devices, especially in APM sensors [15] and resonators [13].

4. In the case of propagation along the grooves, propagation has a form of guiding wave by groove system. For plates corrugated on both sides, changes are not so large as for slant and normal incidence of wave onto the grooves.

Appendix A

Let us consider thin periodically corrugated layer made of piezoelectric material characterised by material tensors e_{qij}, ϵ_{ij}, c_{ijpq} and ρ — mass density. The layer is

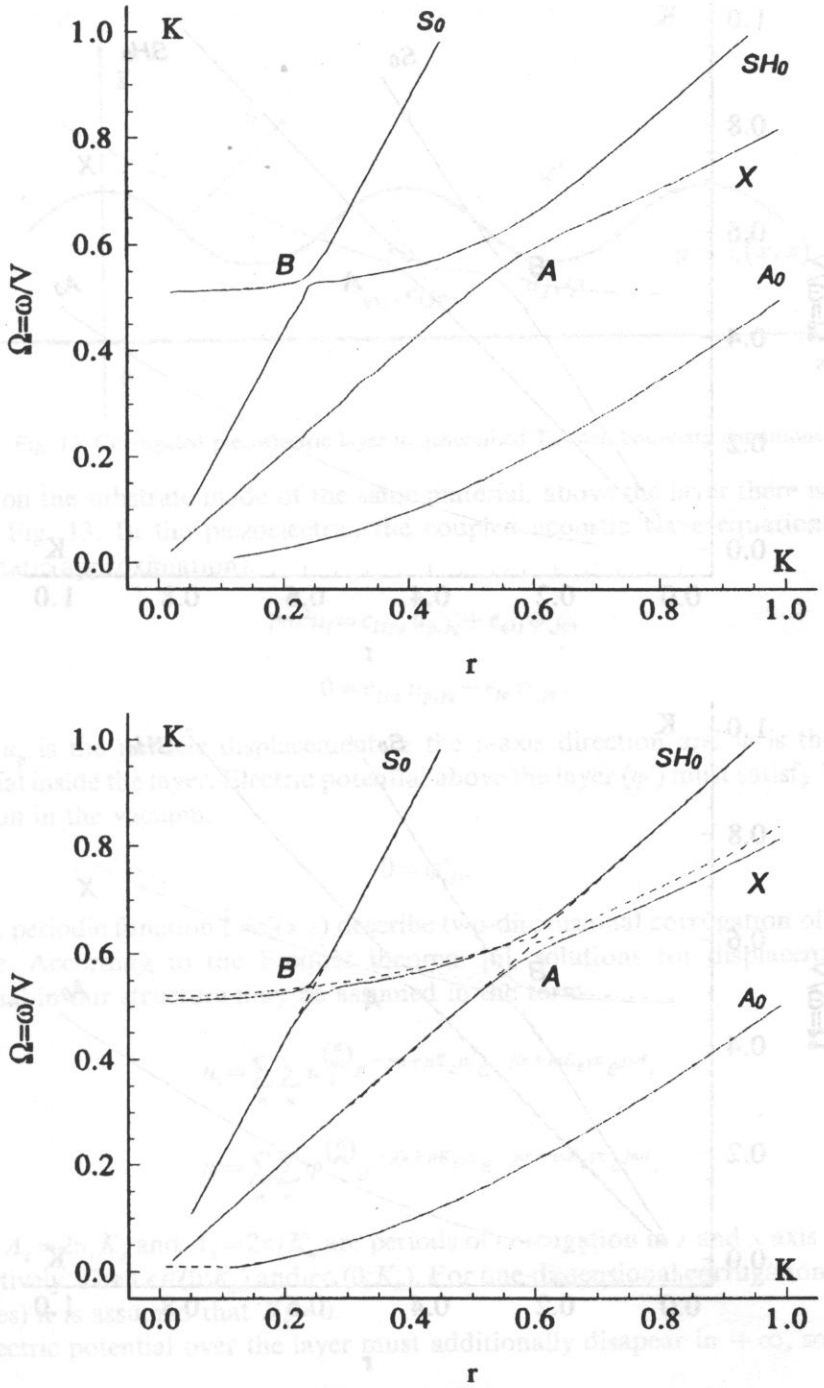

Fig. 11. Dispersion curves, propagation along the grooves ($s=0$)BGO YZ plate, $m=1$ thick. Above: plate corrugated on one side. Below: two-side corrugations phase-shifted by: a) $\psi=0$ — (solid line) and b) $\psi=\pi$ — (dashed line).

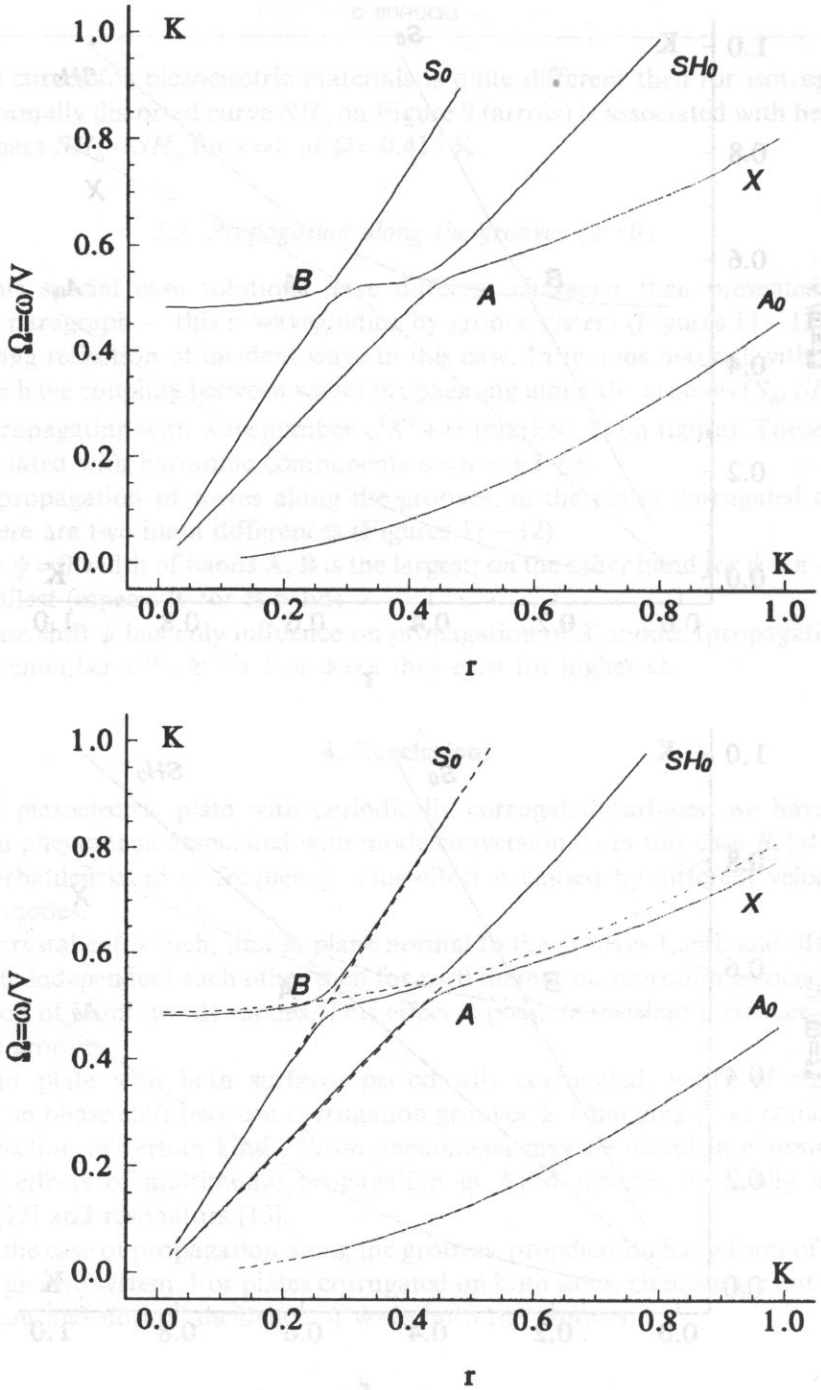

Fig. 12. Dispersion curves, propagation along the grooves $(s=0)LiNbO_3$ YZ plate, $m=1$ thick. Above: plate corrugated on one side. Below: two-side corrugations phase-shifted by: a) $\psi=0$ — (solid line) and b) $\psi=\pi$ — (dashed line).

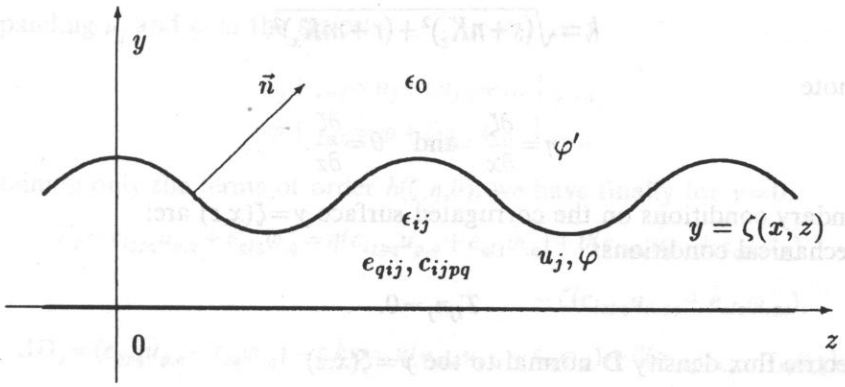

Fig. 13. Corrugated piezoelectric layer in generalised Tiersten boundary conditions.

placed on the substrate made of the same material, above the layer there is vacuum (ϵ_0) — Fig. 13. In the piezoelectric, the coupled acoustic wave equations are (in quasi-static approximation):

$$\rho\omega^2 u_i = c_{ijpq}\, u_{p,jq} + e_{qij}\, \varphi_{,jq},$$
$$0 = e_{jpq}\, u_{p,jq} - \epsilon_{jq}\, \varphi_{,jq}, \tag{A1}$$

where u_p is the particle displacement in the p-axis direction and φ is the electric potential inside the layer. Electric potential above the layer (φ') must satisfy Laplace's equation in the vacuum:

$$0 = \varphi'_{,jj}, \tag{A2}$$

Let periodic function $\zeta = \zeta(x,z)$ describe two-dimensional corrugation of the layer surface. According to the Floquet theorem [6], solutions for displacements and potential in our structure may be assumed in the form:

$$u_i = \sum_n \sum_n u_i^{(n)}_{(m)} e^{-j(s+nK_z)z}\, e^{-j(r+mK_z)x}\, e^{j\omega t},$$
$$\varphi = \sum_n \sum_n \varphi^{(n)}_{(m)} e^{-j(s+nK_z)z}\, e^{-j(r+mK_z)x}\, e^{j\omega t}, \tag{A3}$$

where $\Lambda_z = 2\pi/K_z$ and $\Lambda_x = 2\pi/K_x$ are periods of corrugation in z and x axis direction, respectively. Then $s \in (0; K_z)$ and $r \in (0; K_x)$. For one-dimensional corrugation (periodic grooves) it is assumed that $K_x = 0$.

Electric potential over the layer must additionally disapear in $+\infty$, so:

$$\varphi' = \sum_n \sum_n \varphi'^{(n)}_{(m)} e^{-j(s+nK_z)z}\, e^{-j(r+mK_z)x}\, e^{-ky} e^{j\omega t}, \tag{A4}$$

where:

$$k=\sqrt{(s+nK_z)^2+(r+mK_x)^2}. \tag{A5}$$

Let us note

$$\eta=\frac{\partial\zeta}{\partial x} \quad \text{and} \quad \theta=\frac{\partial\zeta}{\partial z}. \tag{A6}$$

Boundary conditions on the corrugated surface $y=\zeta(x,z)$ are:

• Mechanical conditions:

$$T_{ij}n_j=0. \tag{A7}$$

• Electric flux density **D** normal to the $y=\zeta(x,z)$

$$(D_j-D'_j)n_j=0. \tag{A8}$$

• Electric field **E** tangent to the $y=\zeta(x,z)$

$$\varepsilon_{ijk}(E_j-E'_j)n_i=0, \tag{A9}$$

where n_i are components of vector normal to the surface $y=\zeta(x,z)$

$$\mathbf{n}=[-\eta;\,1;\,-\theta], \tag{A10}$$

and ε_{ijk} is antisymmetric Levi–Civitta symbol.

It is easy to proove that (A9) is equivalent to the continuity of the electric ptoential on the corrugated surface:

$$\varphi'=\varphi \quad \text{at} \quad y=\zeta(x,z) \tag{A11}$$

Let us consider now condition (A8):

$$\text{inside the layer} \quad D_j=D_2-\eta D_1-\theta D_3, \tag{A12}$$

$$\text{in the vacuum} \quad D'_j=D'_2-\eta D'_1-\theta D'_3. \tag{A13}$$

Electric field in the vacuum must disapear in the $+\infty$, so according to the (A4) we have:

$$D'_2=-\epsilon_0\varphi'_{,2}=\epsilon_0 k\varphi' \quad \text{at} \quad y=\zeta(x,z)$$

and finally taking into account (A11) we have for $y=\zeta(x,z)$:

$$D'_jn_j=\epsilon_0\cdot(k\varphi+\eta\varphi_{,1}+\theta\varphi_{,3}), \tag{A14}$$

and, respectivelly:

$$D_jn_j=e_{2pq}u_{p,q}-\epsilon_{2q}\varphi_{,q}-\eta(e_{1pq}u_{p,q}-\epsilon_{1q}\varphi_{,q})-\theta(e_{3pq}u_{p,q}-\epsilon_{3q}\varphi_{,q}). \tag{A15}$$

Mechanical conditions (A7) may be written for $y=z(x,z)$ as follows:

$$T_{ij}n_j=c_{i2pq}u_{p,q}+e_{qi2}\varphi_{,q}-\eta(c_{i1pq}u_{p,q}+e_{qi1}\varphi_{,q})+\theta(c_{i3pq}u_{p,q}+e_{qi3}\varphi_{,q}). \tag{A16}$$

Expanding u_j and φ in the series:

$$u_j \mid_{y=\zeta} = u_j + \zeta u_{j,2} + \ldots \mid_{y=0}$$
$$\varphi \mid_{y=\zeta} = \varphi + \zeta \varphi_{,2} + \ldots \mid_{y=0}$$

and retaining only the terms of order $h(\zeta,\eta,\theta)$, we have finally for $y=0$:

$$T_I = c_{i2pq}u_{p,q} + e_{qi2}\varphi_{,q} = \eta(c_{i1pq}u_{p,q} + e_{qi1}\varphi_{,q}) + \theta(c_{i3pq}u_{p,q} + e_{qi3}\varphi_{,q}) - \zeta(c_{i2pq}u_{p,2q} + e_{qi2}\varphi_{,2q}), \tag{A17}$$

$$\Delta D_2 = (e_{2pq}u_{p,q} - \epsilon_{2q}\varphi_{,q}) - \epsilon_0 k\varphi = \eta(e_{1pq}u_{p,q} - \epsilon_{1q}\varphi_{,q}) + \theta(e_{3pq}u_{p,q} - \epsilon_{3q}\varphi_{,q}) - \zeta(e_{2pq}u_{p,2q} - \epsilon_{2q}\varphi_{,2q}) - \epsilon_0(\eta\varphi_{,1} + \theta\varphi_{,3} + \zeta k\varphi_{,2}) \tag{A18}$$

where $I=6, 2, 4$ for $i=1, 2, 3$ (in shorted notation).

Let us note that for $\zeta \equiv 0$ we have boundary conditions for free (uncorrugated) surface.

Note that derivatives with respect to x, z are known from (A3). Unknown derivatives $(u_{j,2}, \varphi_{,2})$ may be eliminated, taking into account that formulas (A17 – A18) are of first order in h and may be rewriten in the following form ($\delta,\gamma = 1, 3$):

$$c_{i2p2}u_{p,2} + e_{2i2}\varphi_{,2} = -(c_{i2p\delta}u_{p,\delta} + e_{2i\delta}\varphi_{,\delta} + O(h))$$
$$-(e_{2p2}u_{p,2} - \epsilon_{22}\varphi_{,2}) = -(e_{2p\delta}u_{p,\delta} - \epsilon_{2\delta}\varphi_{,\delta} - \epsilon_0 k\varphi + O(h))$$

Thus, if we introduce the symmetric matrix Γ_{ip} by:

$$\Gamma_{ip} \equiv c_{i2p2},$$
$$\Gamma_{i4} = \Gamma_{4p} \equiv e_{2p2} = e_{2i2}, \tag{A19}$$
$$\Gamma_{44} \equiv \epsilon_{22},$$

then we obtain derivatives $u_{j,2}$, $\varphi_{,2}$:

$$u_{\beta,2} = -\Gamma^{-1}_{\beta\alpha}(c_{\alpha 2q\gamma}u_{q,\gamma} + e_{\gamma\alpha 2}\varphi_{,\gamma}) - \Gamma^{-1}_{\beta 4}(e_{2q\gamma}u_{q,\gamma} - \epsilon_{2\gamma}\varphi_{,\gamma} - \epsilon_0 k\varphi), \tag{A20}$$
$$\varphi_{,2} = -\Gamma^{-1}_{4\alpha}(c_{\alpha 2q\gamma}u_{q,\gamma} + e_{\gamma\alpha 2}\varphi_{,\gamma}) - \Gamma^{-1}_{44}(e_{2q\gamma}u_{q,\gamma} - \epsilon_{2\gamma}\varphi_{,\gamma} - \epsilon_0 k\varphi).$$

Because this result holds for all x and z, differentiating with $\delta = 1, 3$ we have a second useful result:

$$u_{\beta,2\delta} = -\Gamma^{-1}_{\beta\alpha}(c_{\alpha 2q\gamma}u_{q,\delta\gamma} + e_{\gamma\alpha 2}\varphi_{,\delta\gamma}) - \Gamma^{-1}_{\beta 4}(e_{2q\gamma}u_{q,\delta\gamma} - \epsilon_{2\gamma}\varphi_{,\delta\gamma} - \epsilon_0 k\varphi_{,\delta}), \tag{A21}$$
$$\varphi_{,2\delta} = -\Gamma^{-1}_{4\alpha}(c_{\alpha 2q\gamma}u_{q,\delta\gamma} + e_{\gamma\alpha 2}\varphi_{,\delta\gamma}) - \Gamma^{-1}_{44}(e_{2q\gamma}u_{q,\delta\gamma} - \epsilon_{2\gamma}\varphi_{,\delta\gamma} - \epsilon_0 k\varphi_{,\delta}).$$

Writing equation of motion for piezoelectric (A1) as follows:

$$\begin{aligned} c_{i2pq}u_{p,2q}+e_{qi2}\varphi_{,2q} &= -(\rho\omega^2 u_i+c_{i\delta p\gamma}u_{p,\delta\gamma}+e_{\gamma i\delta}\varphi_{,\delta\gamma}+ \\ &+c_{i\delta p2}u_{p,\delta 2}+e_{\gamma i}\varphi_{,\delta 2}), \\ e_{2pq}u_{p,2q}-\epsilon_{2q}\varphi_{,2q} &= -(e_{\delta p\gamma}u_{p,\delta\gamma}-\epsilon_{\delta\gamma}\varphi_{\delta\gamma}+ \\ &+e_{\delta p2}u_{p,\delta 2}-\epsilon_{\delta 2}\varphi_{\delta 2}), \end{aligned} \tag{A22}$$

taking into account formula (A21 – A22) we obtain finally:

$$\begin{aligned} c_{i2pq}u_{p,2q}+e_{qi2}\varphi_{,2q} &= -(\rho\omega^2 u_i+c_{i\delta\tilde{p}\gamma}u_{p,\delta\gamma}+e_{\gamma i\delta}\tilde{\varphi}_{,\delta\gamma}+\kappa_{i\delta}\varphi_{,\delta}), \\ e_{2pq}u_{p,2q}-\epsilon_{2q}\varphi_{,2q} &= -(e_{\delta\tilde{p}\gamma}u_{p,\delta\gamma}-\epsilon_{\delta\gamma}\tilde{\varphi}_{\delta\gamma}+\kappa_{4\delta}\varphi_{,\delta}) \end{aligned} \tag{A23}$$

where are introduced the following symbols:

$$\begin{aligned} c_{i\delta\tilde{p}\gamma} &\equiv c_{i\delta p\gamma}-c_{i\delta\beta 2}(\Gamma^{-1}_{\beta\alpha}c_{\alpha 2p\gamma}+\Gamma^{-1}_{\beta 4}e_{2p\gamma})-e_{2i\delta}(\Gamma^{-1}_{4\alpha}c_{\alpha 2p\gamma}+\Gamma^{-1}_{44}e_{2p\gamma}), \\ e_{\delta i\gamma} &\equiv e_{\delta i\gamma}-c_{i\delta\beta 2}(\Gamma^{-1}_{\beta\alpha}e_{\gamma\alpha 2}-\Gamma^{-1}_{\beta 4}\epsilon_{2\gamma})-e_{2i\delta}(\Gamma^{-1}_{4\alpha}e_{\gamma\alpha 2}-\Gamma^{-1}_{44}\epsilon_{2\gamma}), \\ e_{\delta\gamma} &\equiv e_{\delta\gamma}+c_{\delta\beta 2}(\Gamma^{-1}_{\beta\alpha}e_{\gamma\alpha 2}-\Gamma^{-1}_{\beta 4}\epsilon_{2\gamma})-e_{2i\delta}(\Gamma^{-1}_{4\alpha}e_{\gamma\alpha 2}-\Gamma^{-1}_{44}\epsilon_{2\gamma}), \\ \kappa_{i\delta} &\equiv \epsilon_0 k(c_{i\delta\beta 2}\Gamma^{-1}_{\beta 4}+e_{2i\delta}\Gamma^{-1}_{44}), \\ \kappa_{4\delta} &\equiv \epsilon_0 k(c_{\delta\beta 2}\Gamma^{-1}_{\beta 4}+e_{\delta 2}\Gamma^{-1}_{44}). \end{aligned} \tag{A24}$$

Substituting (A21), (A22), (A23) and (A23) to the formulas (A17 – A18), we obtain finally **generalised Tiersten boundary conditions for piezoelectric** in the following compact form:

$$T_I=\zeta\rho\omega^2 u_i+c_{i\delta\tilde{p}\gamma}(\zeta u_{p,\gamma})_{,\delta}+\tilde{e}_{\gamma i\delta}(\zeta\varphi_{,\gamma})_{,\delta}+\kappa_{i\delta}(\zeta\varphi)_{,\delta}, \tag{A25}$$

$$\begin{aligned} \Delta D_2 &= e_{\delta\tilde{p}\gamma}(\zeta u_{p,\gamma})_{,\delta}-\epsilon_{\delta\gamma}(\zeta\varphi_{,\gamma})_{,\delta}+\kappa_{4\delta}(\zeta\varphi)_{,\delta}, \\ &+\epsilon_0(\eta\varphi_{,1}+\theta\varphi_{,3})-\zeta\epsilon_0 k(\kappa_{p\delta}u_{p,\delta}+\kappa_{4\delta}\varphi_{,\delta})+\zeta(\epsilon_0 k)^2\varphi. \end{aligned} \tag{A26}$$

Substituting u_j and φ from (A3) to above formulas, performing differentiation with δ, $\gamma=1, 3$ and collecting terms with the same m and n we obtain generalised Tiersten boundary conditions in matrix form, useful in numerical calculations. Generally they are complicated but for certain piezoelectric materials (i.e. BGO, α-quartz, $LiNbO_3$) they are much simpler due to limited number of non-zero elements of material tensors e_{qij}, ϵ_{ij}, c_{ijpq} [4].

For one-dimensional periodic grooves $K_x=0$, $\eta=0$, $m=0$ and presented above formulas may be written in the form (11).

Acknowledgment

This work is partially supported by KBN Grant 8 S501 001 07.

The author would like to thank prof. Eugene Danicki for his constructive suggestions and kindly remarks which were very helpful during preparation of this article.

References

[1] B.A. AULD, *Acoustic fields and waves in solids*, Wiley, 1973.

[2] E. DIEULESAINT and D. ROYER, *Ondes élastiques dans les solides*, Masson, 1974.

[3] I.A. VIKTOROV, *Rayleigh and Lamb waves*, Plenum Press, 1967.

[4] B.A. AULD, *Acoustic fields and waves in solids*, Wiley 1973.

[5] D.P. MORGAN, *Surface-wave devices for signal proceeding*, Elsevier 1985.

[6] A. PELCZAR, *Wstęp do teorii równań różniczkowych*, [in Polish], v. II, PWN, 1989.

[7] A.I. BELTZER, *Acoustic of solids*, Springer-Verlag, 1988.

[8] E. DANICKI, *Perturbation theory of surface acoustic wave reflection from a periodic structure with arbitrary angle of incidence*, Arch. Mech., **36** (1984).

[9] E. DANICKI, *Rezonator z AFP z konwersją modów* [in Polish], Biuletyn WAT, **37** (1988).

[10] E. DANICKI and D. BOGUCKI, *Wave propagation and scattering in elastic plate with periodically grooved surface*, Arch. of Acoustics, **18** (1993).

[11] A.P. MAYER, A.A. MARADUDIN and W. ZIERAU, *Surface acoustic waves propagation along the grooves of a periodic grating*, Journal of Appl. Phys., **69** (1990).

[12] A.A. MARADUDIN and X. HUANG, *Propagation of horizontal surface acoustic waves parallel to the groves of a random grating*, Journal of Appl. Phys., **70** (1991).

[13] S.G. JOSHI and Y. JIN, *Propagation of ultrasonic Lamb waves in piezoelectric plates*, J. Appl. Phys., **70** (1991).

[14] Y. JIN and S.G. JOSHI, *Electromechanical coupling coefficients of ultrasonics Lamb waves*, JASA, 93, 1993.

[15] F. JOSSE, J.C. ANDLE and J.F. VETELINO, *A theoretical study of acoustic plate modes as biosensing element*, Proc. of 1991 IEEE Ultrasonic Symposium, 1991.